Aircraft crash analysis of the proposed sizewell B containment vessel

Y.Bangash
Faculty of Engineering and Applied Science, Middlesex Polytechnic, Enfield, UK

1. INTRODUCTION

This paper attempts to examine the behaviour of the proposed sizewell B containment vessel under the impact of a multi-role combat aircraft such as a Tornado and Phantom RF-4E. A 60^0 section of the containment vessel is analysed using three dimensional 20 noded isoparametric finite elements adopted in Program CRASH. The impact area under consideration is 28 m^2 which is evaluated from the data obtained from these two aircraft. The vessel is assumed to have unbonded tendons both in the dome and in the barrel wall. The influence of the liner is included in evaluating resistance to the impact.

A Three-dimensional time dependent impact analysis is carried out which incorporates, direct integration concept. The final results obtained include displacements, velocities, accelerations; concrete scabbing, perforation and general cracking. The final damage is shown in a specially prepared post-mortem diagram. The paper has an appendix summarising the constitutive equations for the proposed numerical model.

2. A STEP-BY-STEP DYNAMIC ANALYSIS

The non-linear dynamic finite element analysis reported by Rebora et al (1976) and Bangash (1980) for aircraft crashes. The current analysis reported in this paper takes into consideration the strength of the liner intact initially with concrete by means of lugs and other anchoring devices. The dynamic coupled equations are interprated step-by-step and the response history of the vessel is divided into time increments 'Δt'. If $[M]$ is the mass, $[C]$ and $[K]$ are the damping and stiffness matrices, the equation of motion with specified material properties at time are established.

The equation of motion may be written in incremental form with modified $|C|$ and $|K|$

(1) $$[M]\{\ddot{U}(t)\}+[C_{in}]\{\dot{U}(t)\}+[K_{in}]\{U(t)\} = \{R(t)\}+\{P(t)\}$$

where $\{P(t)\}$ is the initial load $= -\{[\Delta C]^*\{\dot{U}(t)\}+[\Delta K]^*\{U(t)\}\}$ (* indicates for time 0 – t).

Solution at t + Δt

(2) $[M]\{\ddot{U}(t+\Delta t)\}+[C_{in}]\{\dot{U}(t+\Delta t)\}+[K_{in}]\{\Delta R(t+\Delta t)\} + \{\Delta P(t+\Delta t)\}$

$\Delta P(t+\Delta t)$ represents the non-linearity during time increment Δt and is determined by iteration using the stress approach.

(3) $\{\sigma\} = [D_T]\{\epsilon\} - \{\epsilon_0\} + \{\sigma_0\}$

The constitutive law is used with the initial stress and constant stiffness approaches throughout the non-linear and the dynamic iteration. For the iteration

(4) $\{U(t+\Delta t)\}_i = [K_{in}]^{-1} \cdot \{R_{TOT}(t+\Delta t)\}_i$

The strains are determined using

(5) $\{\epsilon(t+\Delta t)\}_i = [B]\{U(t+\Delta t)\}_i$

where [B] strain displacement. The stresses are computed as

(6) $\{\sigma(t+\Delta t)\}_i = [D_T]\{\epsilon(t+\Delta t)\}_i + \{\sigma_0(t+\Delta t)\}_{i-1}$

where $\{\sigma_0(t+\Delta t)\}$ total initial stress at the end of each iteration. All calculations for stresses and strains performed at the Gauss points of all elements.
The initial stress vector is

(7) $\{\sigma_0(t+\Delta t)\}_i = f\{\epsilon(t+\Delta t)\}_i - [D_T]\{\epsilon(t+\Delta t)\}_i$

Using the principle of virtual work, the change of equilibrium and nodal loads $\{\Delta P(t+\Delta t)\}_i$ is calculated as

(8) $$\{\Delta P(t+\Delta t)\}_{iTOT} = \int_{-1}^{+1}\int_{-1}^{+1}\int_{-1}^{+1} [B]^{T''} \{\Delta\rho_0(t+\Delta t)\}_i \, d\xi \, d\eta \, d\zeta$$

$$\sigma_0(t) = \{\sigma_0(t+\Delta t)\}_i = 0$$

$d\xi$, $d\eta$, $d\zeta$ are the local co-ordinates.
The integration is performed numerically at the Gauss points. Effective load vector P(t) is given by

$$\begin{aligned}\{\Delta P(t+\Delta t)\}_{iTOT} = & -[\Delta C(t)_{in}](\{U(t+\Delta t)\}_i - \{U(t)\}) \\ & -[\Delta C(t+\Delta t)]_i\{U(t+\Delta t)\}_i - [\Delta K(t)_{in}](\{U(t+\Delta t)\}_i - \{U(t)\}_i) \\ & -[\Delta K(t+\Delta t)]_i\{U(t+\Delta t)\}_i \end{aligned} \quad (9)$$

Von Mises criteria is used together with transitional factor f^*_{TR} form the basis of the plastic state such that

$$(10) \quad f^*_{TR} = \frac{\sigma_y(t) - \sigma_{y-1}(t)}{\sigma(t+\Delta t)_i - \sigma(t+\Delta t)_{i-1}}$$

The elasto-plastic stress increment will be

$$(11) \quad \{\Delta\sigma_i\} = [D]_{ep} \{\sigma(t+\Delta t\}_{i-1}(1-f^*_{TR})\{\Delta\epsilon\}$$

If $\sigma(t+\Delta t)_i < \sigma_y(t)$, it is an elastic limit and the process is repeated. The equivalent stress is calculated from the current stress state where stresses are drifted they are corrected from the equivalent stress-strain curve.

The residual load vector is calculated as

$$(12) \quad \{R\} = \{P_n\} - \int_V [B]^T \sigma(t+\Delta t)_i \, d\,vol$$

Stresses are checked against cracking criteria to find new cracks. A new secant [D] is built which takes into account the new cracks for changes in modulus of elasticity due to higher compression and also due to additional crushing of concrete. Stresses existing normal to cracks or crushing σ_{CR} are released from the new stresses $\sigma^*(t+\Delta t)_i$

$$(13) \quad \sigma^R(t+\Delta t)_i = \sigma(t+\Delta t)_i - \sigma_{CR}$$

Appendix 1 gives cracking criteria included in the program CRASH.

3. LOADINGS AND VESSEL PARAMETERS

1. Loadings

The load time functions reported by Wolf et al (1978) and Currie et al (1986) for Phantom and Tornado multi-role combat aircraft are summarised in Figure 1. Table 1 gives the material properties. Table 2 shows the vessel parameters given initially for the Size-well B Inquiry (1985).

4. APPLICATION TO SIZEWELL B

Figure 2 shows linear and non linear displacements of the vessel with the final post-mortem given in Figures 3 and 4 for both aircraft.

5. SUMMARY AND CONCLUSIONS

Dynamic analysis under aircraft impact has been carried out using the proposed analysis. The evaluation of the criticality of the containment vessel with the reactor embedded equipment involved a complex interaction of numerous parameters. Upon impact the aircraft can produce two types of effect on the vessel, namely, the local effects and the overall effects. The local effects are characterized by penetration, perforation and backface spalling or scabbing of the vessel material. The overall effects of the aircraft crash on vessel stability are commonly evaluated in terms of the flexural and shear behaviour of the vessel. The aircraft impact or crashes produces a stress wave which is a transitent stress disturbance which travels a finite velocity from the level of application of load. The wave can be longitudinal or dilational parallel to the direction of the impact and transverse or distortional perpendicular to the direction of the impact. Using the Sizewell B parameters and the load-time functions for two aircraft the proposed analysis has been carried out and the results are plotted. During impact the liner in the local area has ruptured. The studs in the local area under impact load have been ruptured. In other areas they have buckled.

REFERENCES

Bangash, Y. 1982. Containment vessel design and practice. Prog. Nucl. Energy, Vol II, No.2, pp 107-181.

Currie et al 1986. Some studies of the response of prestressed containments for PWR to earthquakes, gas cloud explosions and aircraft crash. Nucl. Eng. & Design, pp 173-182.

Rebora et al 1976. Dynamic rupture analysis of reinforced concrete shells. Nucl. Eng. & Design, 37, pp 269-297.

A case for the Size-well B Nuclear Power Station. HMSO 1985.

Table 1 - Design Stress Data.

Conventional Steel	
σy - yield strength	4516 MN/mm^2
Ep = 0.1 E	
Liner 6 mm to 12 mm thickness	
coefficient of linear expansion	10 μM/m ^{0}C
thermal conductivity	41.6 W/m ^{0}C
ϵ_{cu} - ultimate strain	0.0035
E(steel)	200 x 10^3 MN/m^2
E(concrete) - short term	38x10^3 MN/m^2; 34x10^3 MN/m^2(*)
long term	20.7x10^3 MN/m^2
E(soft zones)	0.74E
Ep - plastic modulus	0.476E
Poissons Ratio	0.15 (concrete)
	1.3 (steel)
Coefficient of Thermal expansion of concrete	10x10^{-6}/^{0}C; 12x10^{-6}/^{0}C(*)
Short term specific creep	1830x10^{-9} MN/m^2 ^{0}C
Long term specific creep	2407x10^{-9} MN/m^2 ^{0}C
Minimum crushing strength at 28 days	41.7 MN/m^2

Table 2 : Containment Vessel Parameters

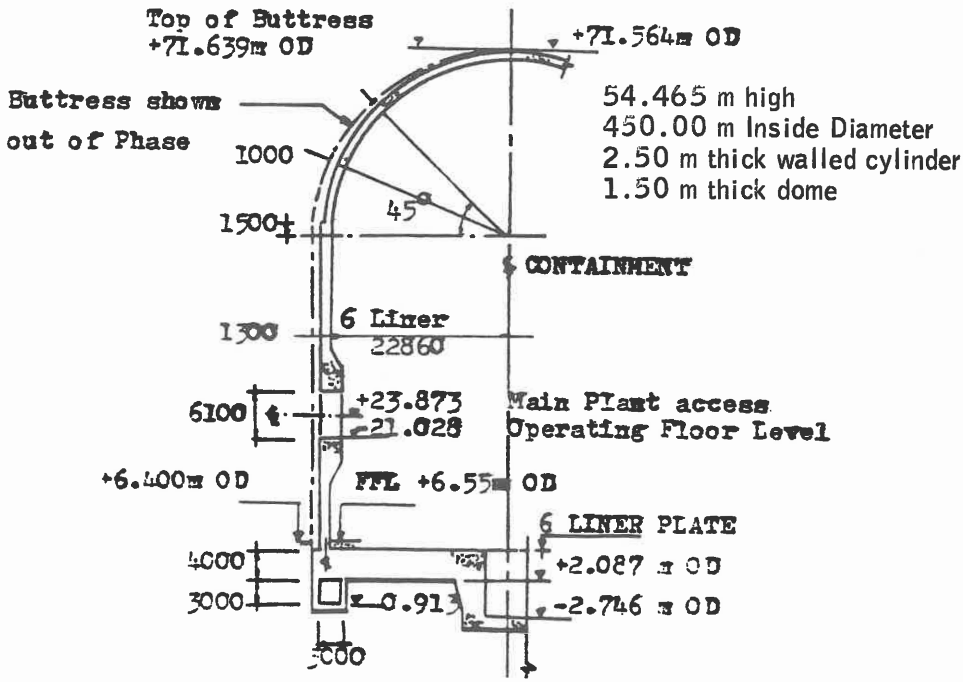

Tendon in wall 6 mm liner.
Wall vertical tendons 76 No.: 11.1 MN Tendons at 972 mm c/c
Wall circumferential tendons 120 No.: 11.1 MN Tendons @ 317 mm c/c

Vetical Section Through Main Plan Access

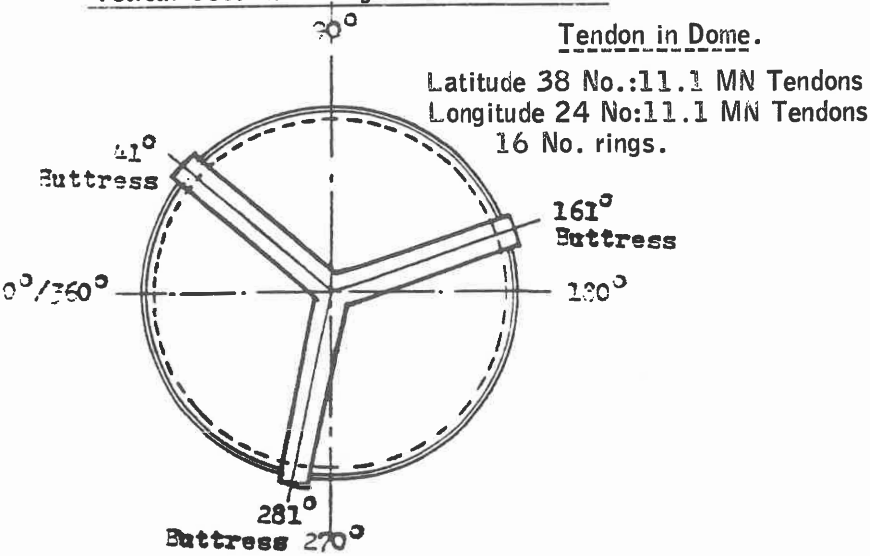

PLAN OF DOME.

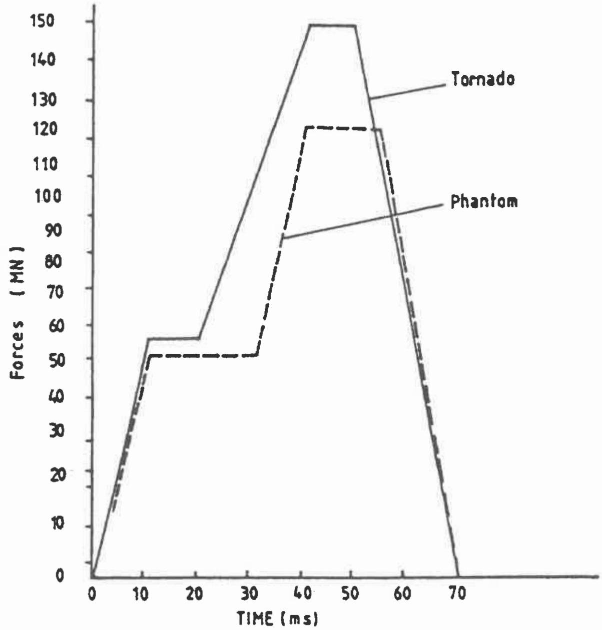

Figure 1 Load time impact function

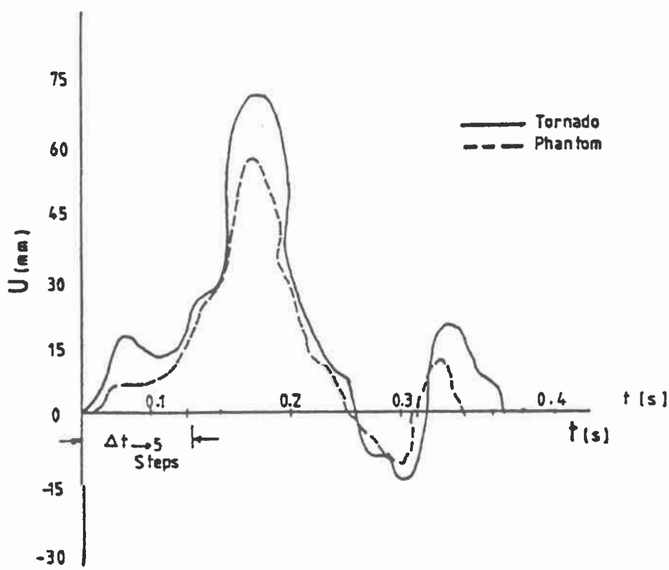

FIGURE 2 : LOAD DISPLACEMENT AS A FUNCTION OF TIME

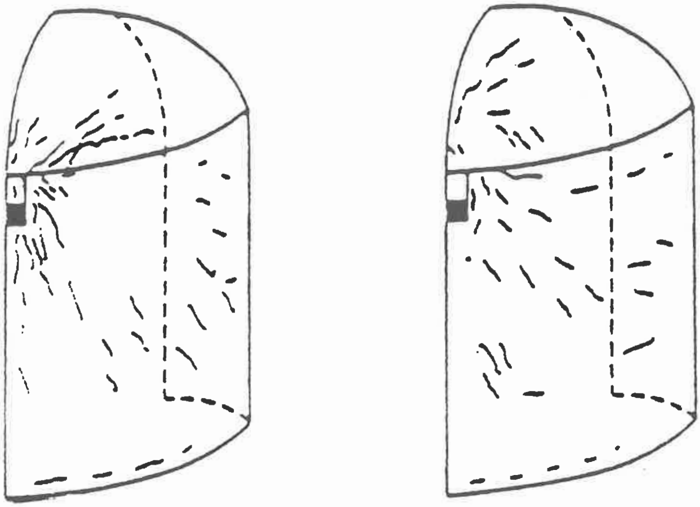

Interior surface. Exterior surface.

Figure 3: Aircraft Phantom Post-Mortem.

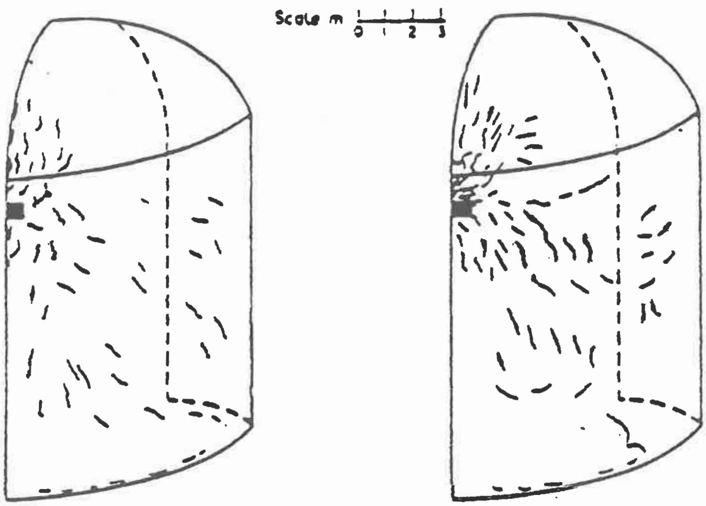

Interior surface. Exterior surface.

Figure 4 : Aircraft Tornado Post-Mortem.

APPENDIX I

Crack indicators NCK (1), NCK (2), NCK (3)

NCK (1) — crack normal to the principal stress '1'
NCK (2) — crack normal to the principal stress '2'
NCK (3) — crack normal to the principal stress '3'

NCK (1) = 0, NCK (2) = 0, NCK (3) = 0 } no cracks

NCK (1) = 1, NCK (2) = 1, NCK (3) = 1 } cracks open.

NCK (1) = 2, NCK (2) = 2, NCK (3) = 2 } cracked closed.

σ, ε — stress strain state at intergrated point
ε_i — principal strains
σ_i — principal stresses $i = 1, 2, 3$
σ_t — limiting tensile strength of concrete
T_ε, T_σ — tranformation matrix

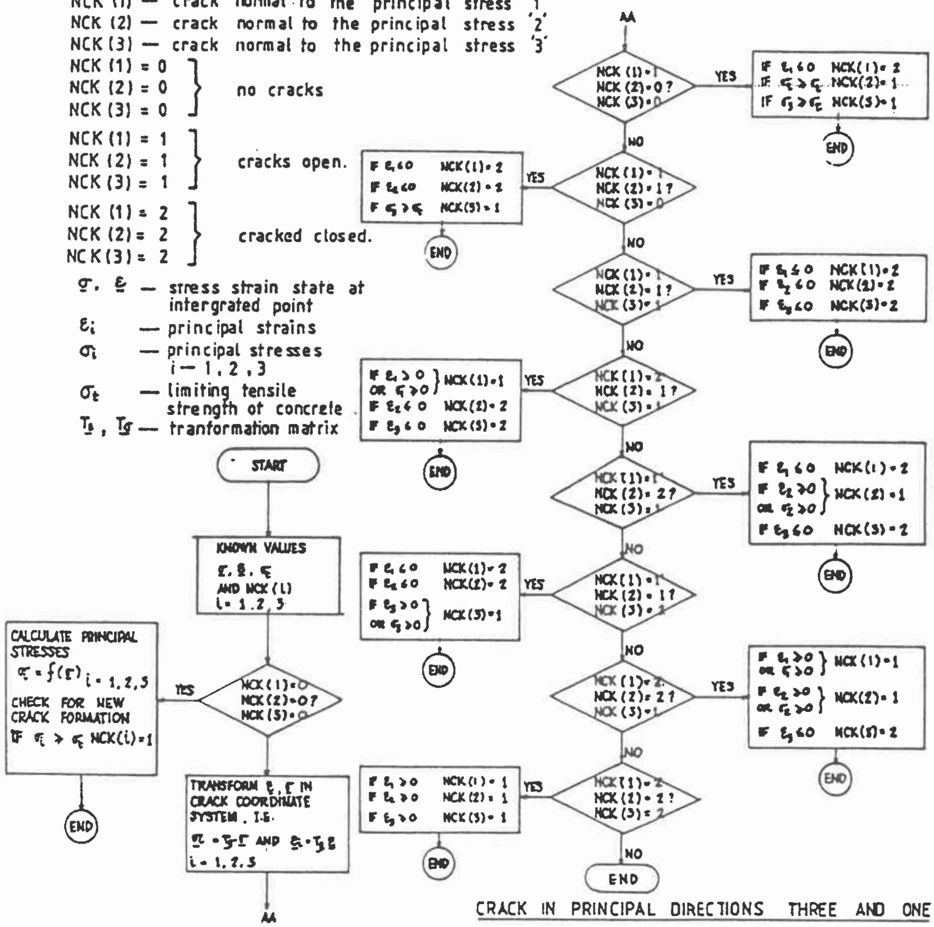

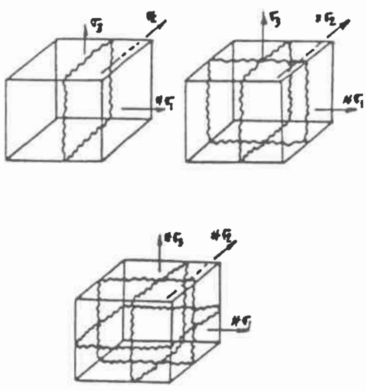

CRACK IN PRINCIPAL DIRECTIONS THREE AND ONE

$$D_{11}^{*} = D_{33}^{*} = D_{12}^{*} = D_{21}^{*} = 0$$

$$D_{13}^{*} = D_{31}^{*} = D_{23}^{*} = D_{31}^{*} = 0$$

$$D_{22}^{*} \quad D_{22} - \frac{D_{12}D_{12}}{D_{11}} - D_{23}\frac{D_{23}}{D_{33}}$$

$$D_{44}^{*} = \beta D_{44}$$

$$D_{55}^{*} = \beta D_{55}$$

$$D_{66}^{*} = \beta D_{66}$$

CRACKS IN ALL THREE PRINCIPAL DIRECTIONS

$$[D^{*}] = [0]$$